In-flight simulation of wake encounters using deformed vortices

D. Vechtel
dennis.vechtel@dlr.de
DLR German Aerospace Center, Institute of Flight Systems
Department of Flight Dynamics and Simulation
Braunschweig
Germany

ABSTRACT

During the decay process the shape of wake vortices changes significantly which has an influence on the encounter characteristics, hence on the encounter hazard. In order to evaluate the influence of vortex deformation on the wake encounter hazard, in-flight simulations with the DLR research aircraft ATTAS were carried out. For a realistic analysis of wake encounters flow fields of matured vortices were generated with large eddy simulations. These flow fields were used for the determination of histories of induced forces and moments acting on the wake encountering aircraft. The force and moment histories were then fed into the equations of motions of the non-linear six degree-of-freedom in-flight simulation of the DLR research aircraft ATTAS. In order to compare different stages of vortex deformation, encounters were simulated in flight with wavy vortices and vortex rings. The most important benefit of the in-flight-simulation is the realistic environment, which enables a realistic assessment of pilots' encounter acceptance. The analysed scenario was of a wake encounter during final approach. The encounter conditions correspond to separation distances of about 4nm and 5nm behind an aircraft of the 'heavy' category. During the encounters the ATTAS was flown under manual control. Altogether 31 encounters were simulated in flight, 9 with wavy vortices and 22 with vortex rings.

Paper No. 3907. Manuscript received 11 September 2012, revised version received 10 April 2013, second revised version received 27 May 2013, accepted 10 June 2013.

https://doi.org/10.1017/S0001924000008654 Published online by Cambridge University Press

The analysis of the results shows that with increasing vortex deformation the encounter impact acts increasingly in all degrees of freedom. Apparently, pilots assess roll-dominated encounters as more dangerous, which is why the unacceptability threshold is higher for encounters with vortex rings than for those with wavy vortices. Besides this unacceptability boundary, a harmlessness boundary can be determined, which seems to be independent from the degree of vortex deformation. This is a most important outcome of the flight test described in this paper. Although, due to the very limited number of flight tests performed, no clear correlation between the pilot ratings and objective measures could be assessed, an acceptance boundary for the roll control ratio could be determined below which the effects of vortex deformation seem to be negligible.

NOMENCLATURE

A/C	aircraft
AIM	aerodynamic interaction model
ATTAS	Advanced Technology Testing Aircraft System
DLR	German Aerospace Center
FbW	fly-by-wire
HFB	Hamburger Flugzeugbau GmbH
ICAO	International Civil Aviation Organisation
ILS	instrument landing system
LES	large eddy simulation
MTOW	maximum take-off weight
RCR	roll control ratio
SHA	simplified hazard area
SHAPe	simplified hazard area prediction
VFW	Vereinigte Flugwerke
VMC	visual meteorological conditions
i_0	initial vortex spacing [m]
n_z	vertical load factor [-]
p	roll rate [°/s]
r	radial distance from vortex [m]
r_c	vortex core radius [m]
t	time [s]
u	longitudinal velocity component [ms^{-1}]
v	lateral velocity component [ms^{-1}]
w	vertical velocity component [ms^{-1}]
x	longitudinal position in vortex axis [m]
y	lateral position in vortex axis [m]
z	vertical position in vortex axis [m]
C_L	lift coefficient [-]
C_D	drag coefficient [-]
C_Y	side force coefficient [-]
C_ℓ	rolling moment coefficient [-]
C_m	pitching moment coefficient [-]
C_n	yawing moment coefficient [-]
N	Brunt-Väisälä-frequency [*1/s*]
N^*	normalised Brunt-Väisälä-frequency [-]

https://doi.org/10.1017/S0001924000008654 Published online by Cambridge University Press

V_T tangential velocity [ms^{-1}]
β sideslip angle [°]
ε eddy-dissipation-rate [m^2/s^3]
ε* normalised eddy-dissipation-rate [-]
Γ vortex circulation [m^2/s]
Γ_0 initial vortex circulation [-]
Γ^* normalised vortex circulation [-]
Φ bank angle [°]

1.0 INTRODUCTION

Wake vortices pose a considerable threat to aircraft. If an aircraft encounters the wake vortices of a preceding aircraft, it may be upset by rapidly induced rolling motion or vertical flight path changes due to downdraughts causing accelerations from which passengers or crew members may be injured or even structural damage of the aircraft may occur. In a few cases, wake encounters even led to the pilot's loss of control so that eventually the encounter resulted in a catastrophic outcome. One example for such a catastrophic event, initially triggered by a wake encounter, is the accident of American Airlines flight 587 on 12 November, 2001. The aircraft crashed into Belle Harbor, New York City, after the vertical stabiliser separated due to strong control of the pilot as a reaction of a wake encounter[(1)].

In order to avoid severe incidents or even accidents due to wake turbulence, the ICAO defined separation minima for approach and departure[(2)] (Fig. 1). These wake vortex related separations have contributed to the prevention of hazardous wake encounters. Nevertheless, quite a number of light or moderate wake encounters occur regularly in airline operations, but usually the consequences are negligible[(3)]. Generally speaking, the present separation distances are commonly accepted to be safe. But in a world with ever increasing air traffic it might be beneficial in the future to revise these separation distances, as they limit airspace and airport capacities[(4)]. But any revision

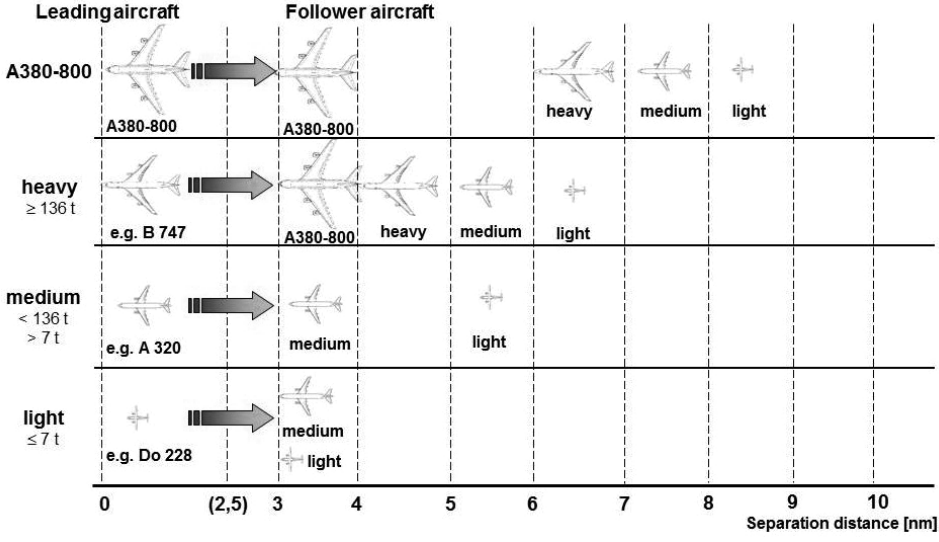


Figure 1. Current ICAO wake turbulence separation minima[(2,4)].

https://doi.org/10.1017/S0001924000008654 Published online by Cambridge University Press

of separation distances must not affect the safety of flight operations negatively. For this reason it is essential to understand the hazard posed by wake vortices. Only if a common understanding exists of which parameters influence the encounter severity, can a revision of separation distances be performed while maintaining an acceptable level of safety as under today's separation rules.

One parameter, often neglected in previous investigations, is the vortex deformation, which occurs during the decay. The key drivers of the deformation are the atmospheric conditions in terms of turbulence and thermal stratification. Previously, for reasons of simplification, wake encounter hazard analyses based on simulations have mostly been performed assuming wake vortices that consist of two straight, counter rotating and infinitely long vortices. However, wake vortices can only be regarded as (nearly) straight right after roll-up. In order to quantify the influence of vortex deformation on the encounter hazard, only a few investigations have been performed. In 2004, Loucel and Crouch[5] were the first who analysed perturbed vortices in flight simulator tests. Until their investigation, all previous wake encounter simulations applied analytical models of straight vortices. In the study of Loucel and Crouch an analytical vortex model was used which takes the perturbed shape of maturing vortices into account. For the early stage of the vortex decay the vortices were modelled as a wavy vortex filament. For later stages, after portions of left and right vortices have linked sequentially, the structure of the vortex lines was modelled by a chain of rings. For a wide range of encounter angles Loucel and Crouch showed a significant reduction of the resulting maximum bank angle during the encounter (in comparison to encounters with straight vortices) due to vortex deformation and the formation of vortex ring structures. The wake encounters were carried out with a B737 simulator, flying with autopilot engaged. Studies like that of Loucel and Crouch can be regarded as relative assessments, comparing encounters against each other based on objective parameters. Such studies are a good basis for comparison of aircraft reaction while encountering straight or deformed vortices. Unfortunately, the influence of vortex deformation can only be analysed in terms of the influence on aircraft reactions, not the resulting subjective encounter hazard. As hazard is a subjective impression of humans, the encounter hazard can hardly be quantified if a study utilises an autopilot.

A common approach for wake encounter hazard assessment is to perform piloted trials. Pilots are probably the best source for advice of what is acceptable or not in terms of threats posed to an aircraft. Piloted studies can usually either be carried out in flight simulators, or in real flight. Analyses of encounters under real flight conditions are the most realistic way to perform a hazard assessment, as the wake vortices are not simulated, including all effect like e.g. vortex deformation inherently. But this method also comprises many uncertainties like undefined scenarios, no reproducibility, or unknown vortex data, which can only be covered by statistics. In order to cover such uncertainties, a large number of encounters need to be performed and analysed. For example, Airbus has conducted more than 1,400 wake encounters in flight trials with various generator aircraft, as well as various encountering aircraft, during cruise flight, as well as approach, in order to support the definition of safe A380 separations[6].

A far less expensive and also safer way to analyse wake encounters with pilots in the loop is to use a flight simulator. However, in this case the degree of reality of the analysed scenario is degraded, as it depends on the accuracy of the wake vortex and aircraft simulation models, which can never match reality under all circumstances. Numerous piloted encounter simulations were recently performed in various projects, e.g. the EU-funded projects S-WAKE[7] and CREDOS[8], as well as the DLR internally funded projects Wirbelschleppe I + II[9] ('Wake Vortex I + II') and Wetter and Fliegen[10] ('Weather and Flying'). In these DLR projects, in-flight simulations with ATTAS were performed. However, most of these encounter simulations were based on simple straight vortex models.

https://doi.org/10.1017/S0001924000008654 Published online by Cambridge University Press

In the framework of the DLR project 'Weather and Flying'' a comprehensive simulator study with pilots in the loop was carried out in a motion-based A330 full-flight simulator[11], applying wavy vortices derived from large eddy simulations[12]. The simulator campaign revealed that, compared to straight vortices, vortex deformation seems to lower the pilot acceptance under manual control. The results of the study indicate that vortex deformation may increase the encounter hazard. Apparently, the higher frequencies of the vortex impact on the encountering aircraft with deformed vortices result in higher demands on the pilot; pilots tended to over control in case of encounters with deformed vortices.

Contrary to the assessment of wake encounters in real flight tests, flight simulators have the great advantage that the encounters are fully definable and repeatable. Due to the fact that all necessary information is available in simulations, including all vortex data, the encounters are fully comparable. This circumstance makes it much easier to develop metrics concerning the encounter hazard, even with a much lower number of encounters. However, although flight simulators are generally able to provide a realistic environment to pilots, they unfortunately cannot give a fully coherent perception of the aircraft motion. Even motion-based simulators cannot give a totally realistic motion impression due to the limited motion envelope of the simulator. But as the motion impression is an important measure for pilots concerning aircraft control, it also influences the pilot's ability to counteract the vortex impact, and hence has an effect on the hazard ratings. Therefore, the results of simulator campaigns (especially using fixed-based simulators) are of limited reliability compared to encounters performed under real flight conditions. This is supported by the experience made in the campaign presented here. Prior to each flight test, the encounters were tested in the fixed-based ATTAS simulator. The pilot ratings gained in these simulator sessions varied from those assessed under real flight conditions, although the encounters were exactly the same. In the simulator 50% of all encounters were not accepted by the pilots, whereas under real flight conditions only 17% of the same set of simulated encounters were not accepted.

In order to further analyse the influence of vortex deformation on the encounter hazard under realistic conditions, DLR Institute of Flight Systems conducted various wake encounter in-flight simulations with the DLR research aircraft ATTAS in the framework of the above mentioned DLR project 'Weather and Flying'. The in-flight simulation comprises advantages of both flight tests with real wake vortices and flight simulator trials. On the one hand, the encounters are simulated and thus can be easily defined and compared, and on the other hand the in-flight simulation provides nearly unconstrained motion and visual cues for the pilots under real flight conditions. For the flight tests with ATTAS, wake vortex flow fields of wavy vortices and vortex rings derived from large-eddy-simulations[11] were used to offer a greater degree of reality possible with this kind of analysis.

In the following sections the phenomenon of vortex deformation during the decay and its dependence on the atmospheric conditions will be explained, followed by a description of the large eddy simulations on which the encounter in-flight simulations were based. Also, the criterion for encounter hazard assessment, which is used in this investigation, will be introduced. The subsequent sections will give an introduction to the in-flight-simulation capability of ATTAS and eventually the flight tests are described and analysed.

1.1 Vortex deformation and atmospheric conditions

As mentioned above, wake vortices can only be regarded as nearly straight right after roll-up. During the vortex decay at first the so-called Crow instability[13] disrupts the vortices and leads to a nearly sinusoidal deformation of the vortices with increasing amplitude in the vertical as well as in the lateral direction. With further increasing amplitude both vortices eventually link at intervals

https://doi.org/10.1017/S0001924000008654 Published online by Cambridge University Press

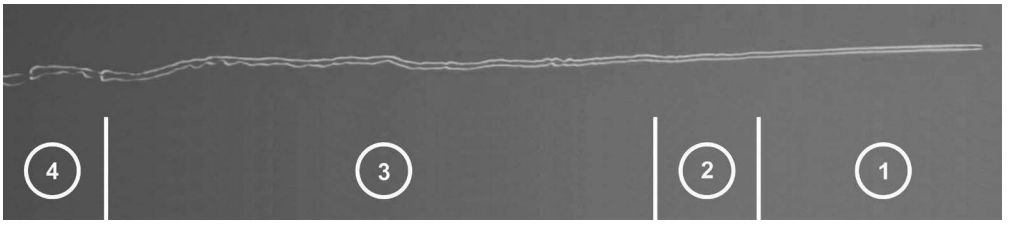


Figure 2. Deformation of wake vortices during decay. (DLR)

and form ring structures. This phenomenon can regularly be observed in the sky, when the contrail of the aircraft makes the wake vortices visible. An example of the possible deformation during the vortex decay is shown in Fig. 2.

In this picture, with the generator aircraft on the right side, the vortices pass through the following stages: (1) initially the vortices are nearly straight and parallel, followed by (2) the onset of Crow instability, (3) sinusoidal deformation (wavy vortices) and (4) first linking and formation of vortex rings. After the formation of vortex rings the circulation decreases significantly in the flight direction of the generator aircraft, whereas in the regions of the vortex line perpendicular to the flight direction, high circulation remains. Figure 3 shows a result of large eddy simulations (LES) as well as a photograph of real vortex rings. The scale of the axes of the numerical results is normalised with the initial vortex spacing b_0, which is usually set to $\pi/4$ of the wing span of the generator aircraft[14]. The colours indicate the normalised circulation Γ^* along the vortex line, which is the current circulation divided by the initial circulation Γ_0. What is most important in this figure is that one can clearly observe the similar shape of the vortex rings in flight and numerical simulation.

The vortex decay and deformation are strongly influenced by the atmospheric conditions, especially in terms of the atmospheric turbulence and thermal stratification[15]. The energy of the atmospheric turbulence is able to increase the vortex decay, as it disrupts the vortices in addition to the normal decay mechanisms. The eddy dissipation rate ε is one important measure for the turbulent energy dissipation, and thus for the vortex decay. The thermal stratification describes the vertical temperature gradient of the atmosphere, and hence affects all vertical motion of the air. Stable thermal stratification leads to a disruption of the vortex structure during the decay, so that the vortices are strongly deformed. Stable stratification means that a vertically displaced fluid particle experiences a force which damps the motion of the particle. Therefore, stable thermal stratification also damps the sinking of wake vortices. A measure for the thermal stratification is the Brunt-Väisälä frequency N which is the frequency at which a vertically displaced fluid particle will oscillate.

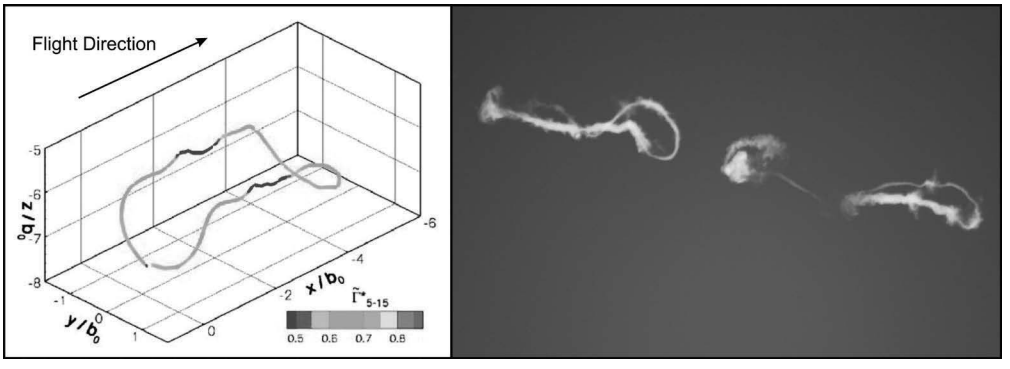


Figure 3. Vortex rings in numerical simulations[12] and in reality. (Mila Zinkova)

https://doi.org/10.1017/S0001924000008654 Published online by Cambridge University Press

Especially in the stage of vortex ring formation, it is clear that the assumption of wake vortices being straight is not valid. Using straight vortices for wake encounter hazard assessment is a strong simplification, which influence the results of the analysis. As vortex deformation has an influence on the conformity of the vortex flow field, it also influences the encounter characteristics. As mentioned above, previous investigations have shown that the characteristics of encounters with deformed vortices can increase the pilot's subjective impression of the encounter hazard compared to straight vortices[11]. Especially in case of wavy vortices, the higher frequencies of the vortex impact on the encountering aircraft (compared to straight vortices) can increase the demands on the pilots, and can therefore lower the acceptance by the pilots[11]. For this reason the assumption of vortices being straight cannot act as a worst case scenario. Vortex deformation should be taken into account for encounter hazard analysis.

1.2 Large Eddy Simulations (LES)

The in-flight encounter simulations with ATTAS were based on flow fields of deformed wake vortices of different vortex ages, derived from large eddy simulations. Generally, LES are able to represent the shape and flow field of wake vortices during the whole decay process in a realistic manner as shown in Fig. 3. Figure 4 depicts the contour of the vortices for the two different vortex ages used in the in-flight simulation.

The generator aircraft in these LES was an aircraft of the ICAO category 'Heavy' in landing configuration, with a current aircraft mass of 190tons and a wing span of 60·3m. The large eddy simulations for this investigation were performed independently from the ATTAS flight tests by the DLR Institute of Atmospheric Physics[12,16]. The LES were conducted with the numerical code LESTUF, which is a 2nd order space and time finite differences code using a staggered grid with a modified Smagorinsky closure scheme. In advance to the actual large-eddy-simulations, simulation runs were performed to adjust the ambient turbulence. When the actual vortex simulation is started the turbulence field is fully developed with a constant dissipation rate and a spectral inertia range following the $k^{-5/3}$-distribution after Kolmogorov[17]. The wake vortices have been initialised with a Lamb-Oseen vortex model[18], which comprises the following equation for the tangential velocity V_T as a function of the circulation Γ, the core radius r_C and the distance from the vortex core r,

$$V_T = \frac{\Gamma}{2\pi r}\left(1 - e^{-1.2544\frac{r^2}{r_c^2}}\right) \quad \ldots (1)$$

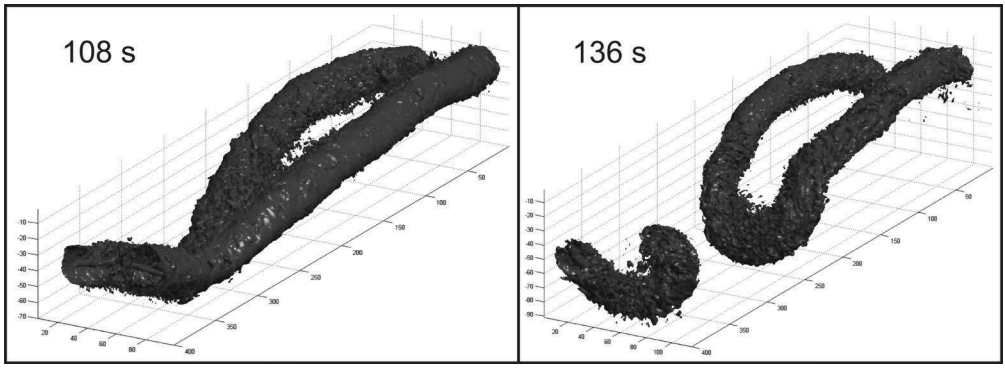


Figure 4. Velocity fields of LES vortices at tage = 108s and 136s.

https://doi.org/10.1017/S0001924000008654 Published online by Cambridge University Press

The outcome of the LES are 3D flow fields for different vortex ages covering the whole decay process. For different atmospheric conditions the three velocity components [*u,v,w*] are given as a function of the spatial position [*x,y,z*] and the vortex age. The dependence on the atmospheric conditions is represented by the normalised eddy dissipation rate ε^*, as a measure of the atmospheric turbulence and the normalised Brunt-Väisälä frequency N*, as a measure of the thermal stratification. Thus, the outputs of the LES are:

$$\left[u, v, w\right]_{flowfield} = f\left(x, y, z, t_{age}, \varepsilon^*, N^*\right) \quad \ldots (2)$$

For the ATTAS flight tests, a normalised eddy-dissipation-rate of $\varepsilon^* = 0{\cdot}23$ (non-normalised eddy-dissipation-rate $\varepsilon = 1{\cdot}10^{-3}$ m^2/s^3) and a Brunt-Väisälä-frequency of $N = N^* = 0$ was chosen. Thus, the atmospheric conditions, on which the LES were based, were moderate turbulence and neutral thermal stratification, which are reasonable values for the lower layers of the atmosphere[19]. Therefore, it is assumed that the deformation of the vortices is representative for final approach altitudes.

The flow field matrices have a length of 400m in flight direction. This length is sufficient for the large eddy simulations, as it covers one wavelength of the Crow instability, which represents one of the predominant mechanisms for vortex decay. However, this length is not sufficient for wake encounter flight simulations. Since, for the LES, the output of one wall equals the input of the opposite wall, the flow field of one vortex age can be connected in series. This way, an infinitely long flow field is formed in the flight direction of the generator aircraft with the repeated shape of the oscillating LES vortices of one vortex age. As the encounter duration is relatively short and the two aircraft fly at similar speeds, it is assumed that the aircraft encounters vortices of constant age and that effects due to vortex decay can be neglected during the encounter. The change of the vortex shape during the encounter is therefore disregarded.

1.3 Subjective encounter hazard rating

Pilot ratings of wake encounter hazard are inevitably purely subjective, as they are based on the pilot's own perception. For quantification of this perception a suitable rating scale is required. DLR developed a rating scale designed for atmospheric disturbances like wake vortices[20] based on a similar rating scale developed by Sammonds and Stinnet in 1975[21]. That scale of Sammonds

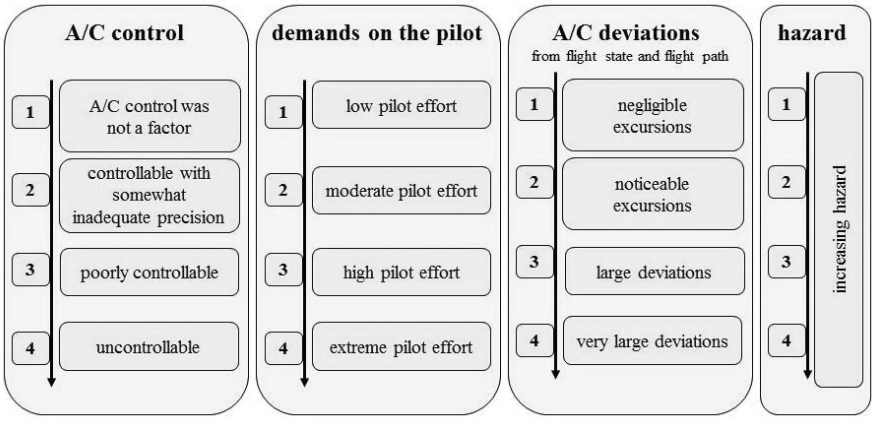


Figure 5. Subjective wake encounter rating scale[20].

https://doi.org/10.1017/S0001924000008654 Published online by Cambridge University Press

and Stinnet was experienced as not sufficient for the desired purpose in previous studies, but the experience with the DLR wake encounter rating scale is good, and several studies showed a good correlation between the pilot ratings and objective encounter data[4,11,22]. The DLR wake encounter rating scale used for the ATTAS in-flight simulations is depicted in Fig. 5.

As can be seen in Fig. 5 the pilots have to rate four different categories independently on a scale from 1 to 4: aircraft control, demands on the pilot, aircraft deviations and the overall hazard. The overall hazard rating is treated independently from the other rating categories, as e.g. a go-around has to be rated with '4' in aircraft deviations by definition, as the deviations from the intended flight path are certainly 'very large' in that case, whereas the manoeuvre itself is not necessarily hazardous. Contrary to the other rating categories, which are indeed subjective but correlate to objective measures (e.g. deviations from the desired flight path), the overall hazard rating is a purely subjective impression and might differ between different pilots. However, if at least one of the four rating categories is rated with '4' by the pilots, the encounter is defined to be unacceptable.

In this study the use of this rating scale has been modified with respect to previous studies. Recently, the ratings were used to solely distinguish between acceptable (no rating of '4') and unacceptable encounters (at least one category rated with '4')[11,22]. This boundary is the so-called unacceptability boundary. The experience made in those past investigations motivated a slightly different approach for the evaluation of the ATTAS in-flight simulations. Those studies showed that, if the average rating of all four rating categories is below 2, the encounter is harmless in the pilots' opinion and hardly distinguishable from ordinary atmospheric turbulence. Average ratings above 2, but without a rating of 4, are defined by the experimenter to be still acceptable, but the experience shows that for those considerable encounters the ratings strongly depend on the individual perception of the pilot. For this reason a second boundary shall be introduced (besides the unacceptability boundary), which is the harmlessness or acceptability boundary. In between this acceptability boundary and the unacceptability boundary an area is located, in which some pilots would rate the encounter acceptable and some would not. This approach is described in Fig. 6.

Such an approach is a conservative way to assess the encounter hazard, but in the author's opinion it is a reasonable approach to define what is definitely acceptable and what is definitely unacceptable.

1.4 The roll control ratio – a metric for wake encounter hazard assessment

For a comprehensive hazard assessment the subjective encounter ratings need to be correlated with objective metrics, which describe the encounter hazard on an objective level. By means of such

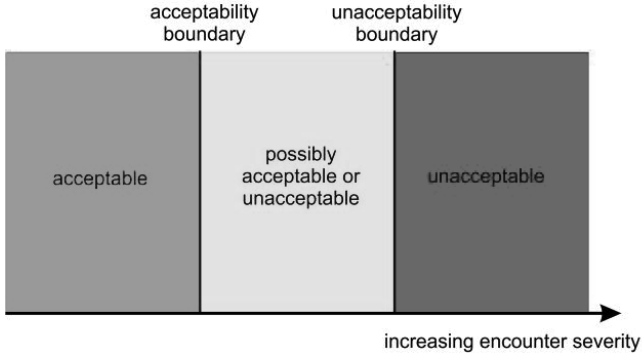


Figure 6. Wake encounter severity levels[23].

https://doi.org/10.1017/S0001924000008654 Published online by Cambridge University Press

objective metrics boundaries could be found between acceptable and unacceptable encounters. The metric should have a strong correlation between the encounter severity (pilot's hazard rating) and measurable parameters, should be easy to determine and meaningful, and the limit value for definition of what is acceptable and what is unacceptable should be aircraft independent[24].

During a landing approach, aircraft mostly fly on nearly parallel flight paths. In such case the predominant impact of a wake encounter is rolling motion induced on the encountering aircraft. For this reason it is useful to choose a criterion for hazard assessment which takes the rolling motion into account. The so-called roll control ratio (RCR) is one hazard metric, which fulfils nearly all the above mentioned requirements. The RCR is the ratio of the rolling moment induced by the vortices and the maximum rolling moment of the rolling motion control motivators (maximum roll control power)[25].

$$RCR = \left| \frac{C_{\ell,ind}}{C_{\ell,CTRL,\max}} \right| \quad \ldots (3)$$

Thus, the RCR is indeed not aircraft independent as it requires knowledge concerning the aircraft roll control power. Unfortunately this value might not be accessible for many existing aircraft. For this reason DLR developed the so-called SHAPe approach, in order to estimate the roll control power on a conservative level. SHAPe (simplified hazard area prediction) utilises statistical data from various aircraft to evaluate the maximum roll control power based on the maximum take-off weight MTOW. Thus, for unknown aircraft data SHAPe can be used for calculation of the roll control ratio. The RCR showed the capability to serve as an appropriate hazard metric in past investigations[11,22]. For this reason the RCR is used as the main criterion for the analysis of the wake encounter in-flight simulation with the ATTAS.

If an RCR boundary could be found, below which wake encounters can be regarded as harmless, areas surrounding the vortices can be defined, which have to be avoided for safe flight (simplified hazard areas SHA[26]). Figure 7 depicts a typical RCR distribution around two wake vortices for a specific aircraft pairing.

For a specific threshold in RCR, beyond which encounters may be hazardous, the hazard area can be defined by the two lengths '*a*' and '*b*'. If a hazard limit based on RCR is chosen small enough, it

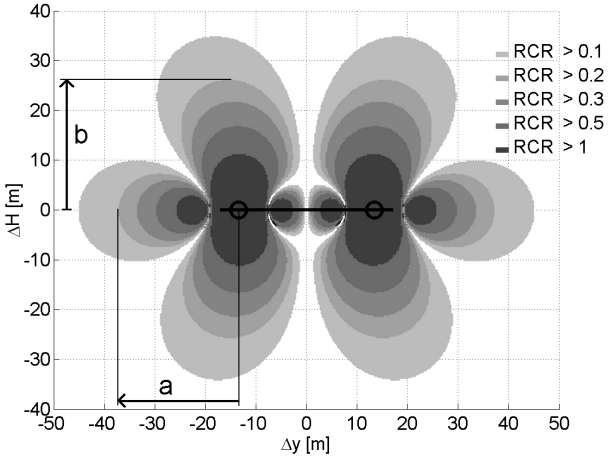


Figure 7. Typical RCR distribution for a fixed-wing aircraft in a vortex pair.

https://doi.org/10.1017/S0001924000008654 Published online by Cambridge University Press

also covers all other effects of roll-dominated wake encounters affecting the encountering aircraft (e.g. downdraught). This was shown in previous investigations, which also revealed an acceptance boundary of RCR = 0·2 for straight vortices[22] covering all encounter impacts. As this limit value was assessed for straight vortices only, it needs to be further investigated whether this boundary is also applicable to deformed vortices. The previously mentioned simulator study in an A330 full-flight simulator using wavy vortices and straight vortices indicated that the unacceptability boundary may vary with the degree of vortex deformation. This quantification is one of the major goals of the in-flight simulation study with ATTAS.

2.0 THE DLR IN-FLIGHT SIMULATOR ATTAS

DLR operated the research aircraft ATTAS (Advanced Technologies Testing Aircraft System) for a period of 27 years between 1986 and 2012. ATTAS was based on the VFW 614, a German civil transport aircraft developed in the late 1960s with maiden-flight in 1971. The VFW 614 was a short-haul twin-engine jet aircraft designed for 44 passengers with a wing span of 21·5m and a length of 25m[27]. Altogether, only 19 aircraft of this type were built, and since 1998 ATTAS was the only VFW 614 still remaining in service. DLR had already gained in-flight simulation experience since 1972, when a HFB 320 Hansa, the first German business jet, was introduced as an in-flight simulator. In 1986 the HFB 320 Hansa in-flight simulator was then replaced by the more sophisticated ATTAS (Fig. 8).

Due to its size, its relatively spacious cabin, its additional load capacity and its flight characteristics, the VFW 614 was an ideal flying test-bed for various applications[27]. Fully fuelled the ATTAS was able to carry a load of 3·5tons of test equipment. In order to directly control almost

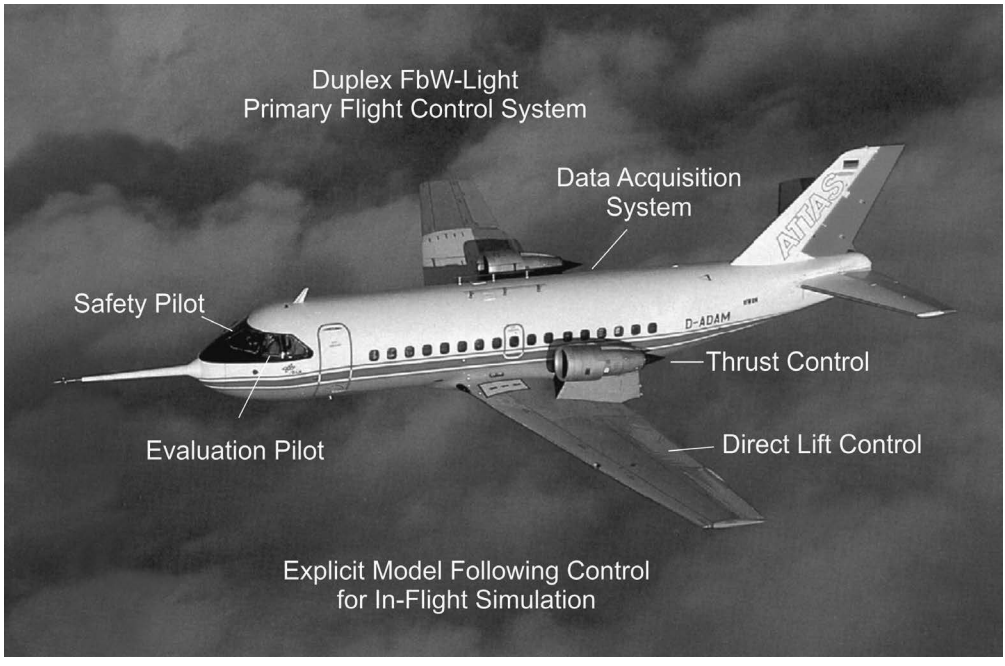


Figure 8. The DLR research aircraft ATTAS.

https://doi.org/10.1017/S0001924000008654 Published online by Cambridge University Press

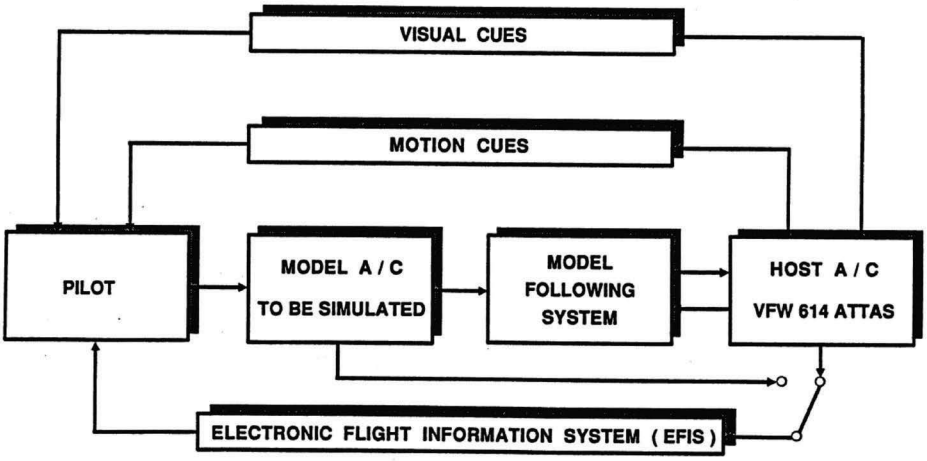


Figure 9. Architecture of ATTAS in-flight simulation[29].

all degrees of freedom, the ATTAS was equipped with six additional direct lift control flaps, which were located at the trailing edge of the high-lift flaps. With these flaps it was possible to influence the lift very fast, and thus five of the six degrees of freedom could be controlled directly. Additional to the conventional mechanical flight control system, ATTAS was also equipped with an electronic flight control system (fly-by-wire). With the electronic flight control system engaged for flying by the experimental pilot for the in-flight simulation, the safety pilot could revert back to the mechanical flight control system at any time.

2.1 In-flight simulation capability of ATTAS

The aim of in-flight simulation is to represent the behaviour of a model-based virtual aircraft using a specific host aircraft to provide nearly unconstrained motion and visual cues for the pilot under real flight conditions[28]. As mentioned above, ATTAS is equipped with additional control surfaces, the direct lift control flaps, so that it is able to directly control five of the six rigid-body degrees of freedom. The in-flight simulation is based on a non-linear six-degrees-of-freedom aircraft simulation running on-board the ATTAS, which is followed by model following controller. This model following controller consists of feed-forward and feed-back control loops and comprises an inverted simulation model of the ATTAS host aircraft. The model following controller calculates the necessary control surface deflections to make the real VFW 614 ATTAS follow the motion of the simulated aircraft. Figure 9 shows the architecture of the ATTAS in-flight simulation.

The model aircraft to be simulated can be arbitrary, but the dynamics of the model have to be within the envelope of dynamics of the host aircraft. In case of the in-flight simulation described here, the simulated aircraft was also the VFW 614. Once the in-flight simulation is engaged the experimental pilot no longer controls the real aircraft directly, but the pilot's control inputs are fed into the non-linear aircraft simulation. Via the model following controller, the real ATTAS host aircraft is then forced to follow the motion of the simulated aircraft.

2.2 In-flight simulation of wake encounters

Through the in-flight simulation, the real aircraft is able to encounter a simulated wake, so that the impression is given to the experimental pilot of a real wake encounter. Thus, during the encounter

https://doi.org/10.1017/S0001924000008654 Published online by Cambridge University Press

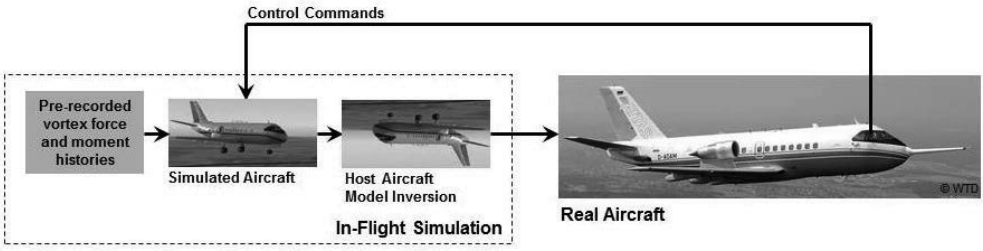


Figure 10. Schematic description of the ATTAS in-flight simulation of wake encounters.

simulation the experimental pilot has to counteract the simulated wake impact on the aircraft as during a real encounter. A schematic description of the wake encounter in-flight simulation with ATTAS is depicted in Fig. 10.

The technique to hit the wake in a reproducible way used in this study is called 'time-fixed' encounter. This is a method to expose the aircraft to a wake vortex upset, which uses pre-computed and recorded force and moment histories for a defined flight path. These time histories are used in the simulation instead of calculating them in real-time depending on the relative position to the vortex (so-called 'space-fixed' encounters). The advantage of this method is that the disturbance is fixed no matter what the pilot does so any scatter in the aircraft reactions can only be due to variation in the control inputs. Indeed, this method is a simplification, as in reality pilot control inputs and flight path variations have an effect on the wake impact. However, the higher degree of reality of space-fixed encounters is also a disadvantage for the analysis, as the aircraft will likely not hit the vortex at the desired position. These uncertainties can only be covered by statistics, so that a large number of tests need to be performed. For this reason the method using time-fixed encounters has proven to be useful when comparing the control inputs and hazard ratings of different pilots on the same defined disturbance for a limited set of experimental data[11,22,26]. The error made by using time-fixed vortices is assumed to be small as long as deviations between the predefined track and the track flown in the experiment are small.

For the computation of vortex forces and moments no dynamic aircraft simulation is required. A delta model called aerodynamic interaction model (AIM) calculates the incremental forces and moments for the specific aircraft type using the strip method[30]. Here, the lift and side-force generating surfaces are subdivided into sections, for which the vortex influence is determined. For each strip an additional angle of attack, or an additional angle of sideslip, due to the vortex flow-field are calculated. By means of aerodynamic derivatives, the resulting three additional forces and with the respective lever arm of each strip the resulting three moments, are calculated. This

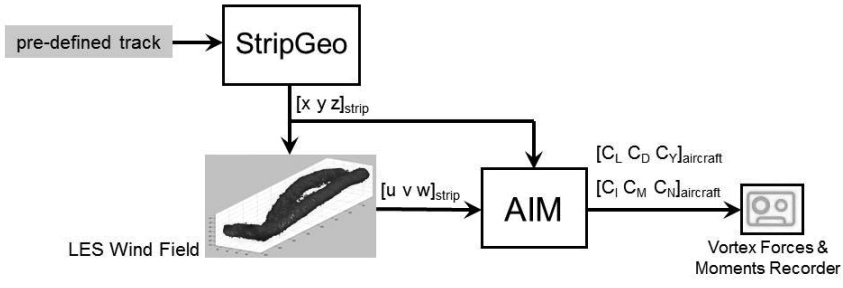


Figure 11. Calculation of vortex forces and moments by means of the aerodynamic interaction model.

https://doi.org/10.1017/S0001924000008654 Published online by Cambridge University Press

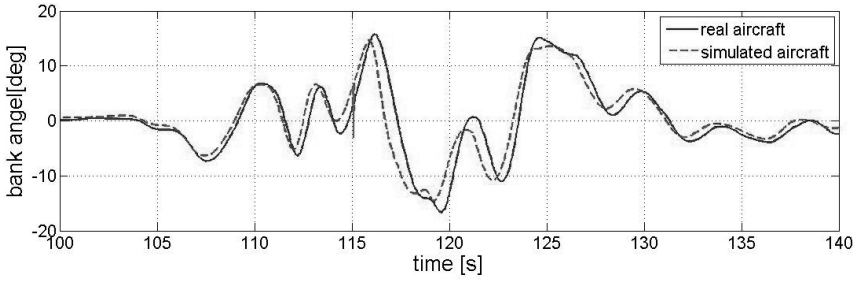


Figure 12. Comparison of bank angle for real and simulated aircraft during an encounter.

method was deemed feasible by Barrows[31], verified against wind-tunnel tests by de Bruin[32] and validated using real flight test data by Fischenberg[33] and Jategaonkar[34]. A schematic description of the vortex forces and moments calculation is shown in Fig. 11.

In order to record forces and moments due to the vortices, the AIM was carried out on different pre-defined tracks through the vortex flow field. Depending on the envisaged nominal roll control ratio the lateral position of the track differs. The track for the recording was a three degrees descent left or right of the wake vortex centre line with the same azimuth. The strip geometry calculation computes the spatial position of each strip along the desired flight path. With the respective velocity components from the vortex flow field the AIM calculates the resulting forces and moments as non-dimensional coefficients. However, for the in-flight simulation the force and moment coefficients need to be transferred into dimensional forces and moment to be fed into the equations of motion of the dynamic aircraft simulation.

The pre-recorded sets of force and moment histories were implemented in the in-flight simulation software. Depending on a specific activation altitude, the force and moment histories were played back in the simulation. The analysis of the recorded data shows a good conformity of the motion of the simulated and the real aircraft. The behaviour of the real ATTAS represented the simulated encounter situation very realistically, which is shown in Fig. 12 for the bank angle. The figure shows a comparison between simulated and real aircraft during the encounter. One can see that the real aircraft follows the motion of the simulated aircraft very well.

3.0 ACCOMPLISHMENT OF FLIGHT TESTS

All wake encounters were simulated during final approach. The pilot's task was to perform an ILS approach under VMC with the aim to land the aircraft. However, landing was not intended during the tests, but instead each approach was finished with a go-around after completion of the test a few hundred feet above ground, in order to circle and perform the next approach.

Depending on pre-defined but differing activation heights the vortex-induced forces and moments were played back time-fixed after reaching this specific height. The heights when the encounter started varied between 650ft and 1,050ft above ground depending on the vortex strength. As mentioned above, the flight tests comprised simulated encounters of vortices of two different ages. The vortex ages correspond to deformed vortices prior to linking (wavy vortices) and vortex rings. As the ATTAS flight tests are of very limited number, only those encounters with LES-generated vortices were simulated. In-flight simulations with straight vortices were performed in various previous flight test campaigns with ATTAS. The results of those studies are able to serve as a basis for comparison.

https://doi.org/10.1017/S0001924000008654 Published online by Cambridge University Press

Under the given atmospheric conditions, and for typical approach speeds, the analysed vortex ages correspond to separation distances of about 4nm for the wavy vortices and 5nm for the vortex rings. As ATTAS is in the 'medium' category of the ICAO wake vortex aircraft categories, it is to be separated by 5nm behind a heavy aircraft. Hence, the encounter scenario of the wavy vortices is of less relevance for ATTAS from the operational point of view, but is nevertheless interesting to analyse for hazard assessment. Comparison with encounters using straight vortices can be made by means of results gained in previous investigation[22].

During and after the encounter the pilot task was to stabilise the aircraft and to pursue the ILS approach. If the pilots were not able to stabilise the aircraft, or felt like they could not safely continue landing after the encounter, they should initiate a go-around immediately. The pilot's decision to perform a go-around was based on common limitations known from airline operations (e.g. bank angle or glide slope exceeding specific values), or if the pilots subjectively felt unsafe during the encounter. If the pilots were sure that they could safely continue the landing after the encounter, the approach was resumed and the experimental sequence was finished. Eventually each approach was finished with a go-around shortly before touch-down, in order to circle and to perform the next approach. After each test the pilots had to rate the encounter by means of the encounter rating scale depicted in Fig. 5. All-in-all 31 encounters were simulated in-flight during six flights with three different experimental pilots.

4.0 RESULTS

As mentioned in section 1.4 one goal of the in-flight simulations was to verify a wake encounter acceptance boundary based on the roll control ratio (RCR) for deformed vortices. For this reason the analysis is performed using this metric. Contrary to previous analyses the pilot ratings should not solely serve as a basis to determine a boundary beyond which encounters are clearly unacceptable, but also to determine a harmlessness boundary as described in section 1.3. The following figures include all encounters, but do not distinguish between the different pilots.

The colour coding in the following figures depicts the pilot rating of each encounter. Green marks mean that the average rating of the respective encounter is below a value of 2. As described in section 1.3, the experience made during the flight tests showed that those encounters are definitely harmless. The encounters which are still acceptable (i.e. no rating of 4), but with an average rating greater than 2, are marked yellow. Those encounters are indeed still acceptable, by definition, but result in an increased pilot workload and noticeable flight state deviations. The encounters with one or more rating categories rated with 4 are unacceptable by definition. In the figures these are marked in red ('At least one Rating = 4').

Figures 13(a) and (b) depict the results from flight tests in terms of the maximum roll control ratio, which occurred during the encounter, and the actual encounter height above ground. The encounter height shown in Fig. 13 is the height where the maximum RCR occurred during the encounter. Fig. 13(a) shows the results of encounters with wavy vortices, whereas Fig. 13(b) shows those with vortex rings.

One can clearly observe in Fig. 13 that the boundary between the area with only green marked encounters and the area with yellow marked encounters (harmlessness boundary) is in a similar range for wavy vortices and vortex rings (RCR $\approx$ 0·25 to 0·3). On the other hand, the unacceptable encounter with the lowest RCR value (unacceptability boundary) is in a very different range of RCR for wavy vortices and vortex rings. The unacceptability boundary for wavy vortices is at an RCR of approximately 0·5, whereas those encounters with vortex rings have all been accepted below an RCR of about 1.

https://doi.org/10.1017/S0001924000008654 Published online by Cambridge University Press

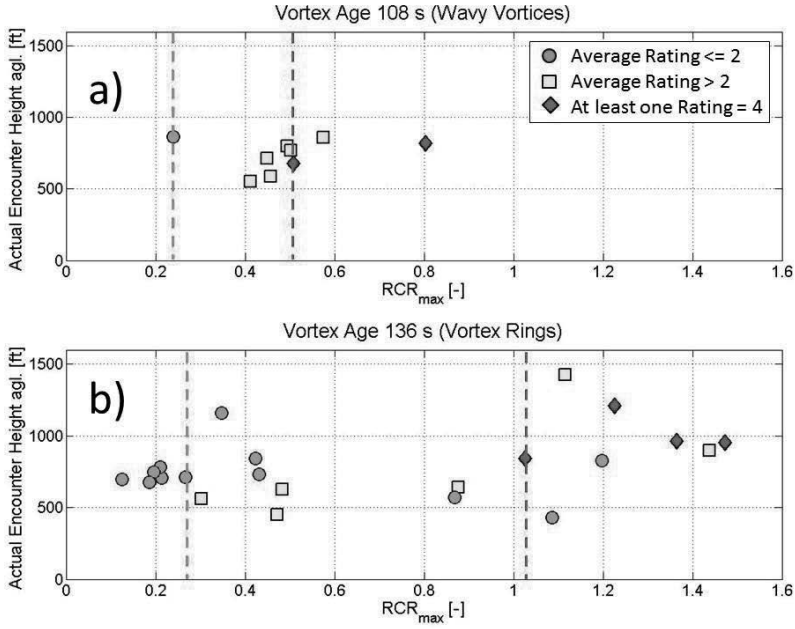


Figure 13. Ratings of encounters with wavy vortices (a) and vortex rings (b).

The qualitative impression experienced during the flight tests is that the impact of the vortices acts increasingly on all axes with increasing vortex deformation. Encounters with wavy vortices are dominated by induced rolling motion, whereas encounters with vortex rings also show remarkable impact in the yawing axis and vertical flight path. Nevertheless, vortex rings may also induce significant rolling moments depending on the position where the vortices are being hit. For this reason the roll control ratio is also considered a meaningful hazard metric for encounters with vortex rings. The evaluation of the pilot ratings supports this impression quantitatively.

It is evident that the in-flight simulation is only able to represent encounters up to a roll control ratio of 1. Above RCR = 1 the dynamics of the host aircraft are not sufficient to represent the encounter. For this reason the maximum envisaged RCR of the encounters was 1·1. The larger RCR values for the vortex rings in Fig. 13 can be explained by the way how the force and moment histories are implemented in the in-flight simulation. As the equations of motion of the aircraft simulation require dimensional input, the corresponding computation of the roll control ratio, which is calculated in a non-dimensional manner, is sensitive to speed deviations. If the speed maintained by the pilots during the flight experiment differs from the nominal airspeed of the force and moment history generation, the calculated roll control ratio must inevitably differ from the envisaged maximum RCR. In those cases with large RCR values (>1·2) the pilot encountered the vortices at lower airspeed, so that the RCR values increased. However, the dimensional vortex induced forces and moments during the encounter did not change due to the speed variation.

It might also be surprising that pilots rated encounters with RCR values greater than 1 as acceptable. This can be explained by the encounter characteristics. In all figures shown here the maximum RCR value which occurred during the encounter is depicted. But especially during encounters with vortex rings these maximum values occurred only for very short periods of time, so that the induced rolling moment could not significantly affect the aircraft motion.

https://doi.org/10.1017/S0001924000008654 Published online by Cambridge University Press

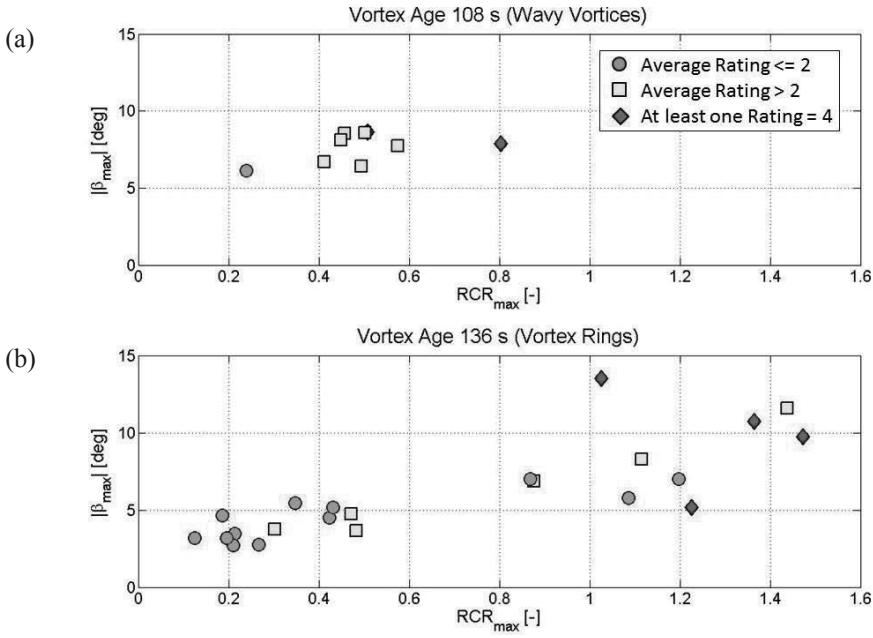


Figure 14. Resulting maximum sideslip angle during encounters with wavy vortices (a) and vortex rings (b).

Figure 14 depicts the resulting maximum absolute sideslip angle during the encounters with wavy vortices and vortex rings.

One can observe in Fig. 14 that, for large RCR values, the resulting sideslip angle is larger for vortex rings than for wavy vortices. However, the lack of encounters with comparably large RCR values for wavy vortices does not clearly verify that encounters with wavy vortices may not result in such large sideslip angles, as did occur with vortex rings. But the pilot ratings indicate that pilots might accept relatively large sideslip angles, and that the sideslip angle is not the main factor for the respective rating. This fact might not be surprising as the experimental pilot does not have a numerical indication of the sideslip angle in the cockpit. For this reason the pilot is not able to quantify the maximum sideslip angle which occurred during the encounter, but only qualitative, hence subjective impressions, from the lateral acceleration cues. Figure 14 does not, therefore, show a clear correlation between the sideslip angle and the pilot ratings.

Contrary to the sideslip angle, the vertical load factor shows that downwash has a more considerable impact for vortex rings rather than for wavy vortices. Figure 15 shows that even for small RCR values larger load factors occurred during the encounters with vortex rings. With vortex rings a Δn_z of 0·6 occurred at an RCR of 0·2, whereas for wavy vortices only a Δn_z of 0·3 occurred at a similar RCR. However, as for the sideslip angle the pilot ratings indicate that pilots might also accept relatively large vertical load factors during encounters. Also, the load factor does not clearly correlate with the pilot ratings, hence it might not be a main factor for the pilots' ratings.

After most unacceptable encounters, the pilots stated that the main factor for the rating was the impact in the roll axis. This can be observed for the roll rate, which is shown in Fig. 16. The results show that all unaccepted encounters were affected with a large roll rate. Also, Figure 16 indicates that for comparable RCR values encounters with wavy vortices may result in slightly larger roll rates than those with vortex rings.

https://doi.org/10.1017/S0001924000008654 Published online by Cambridge University Press

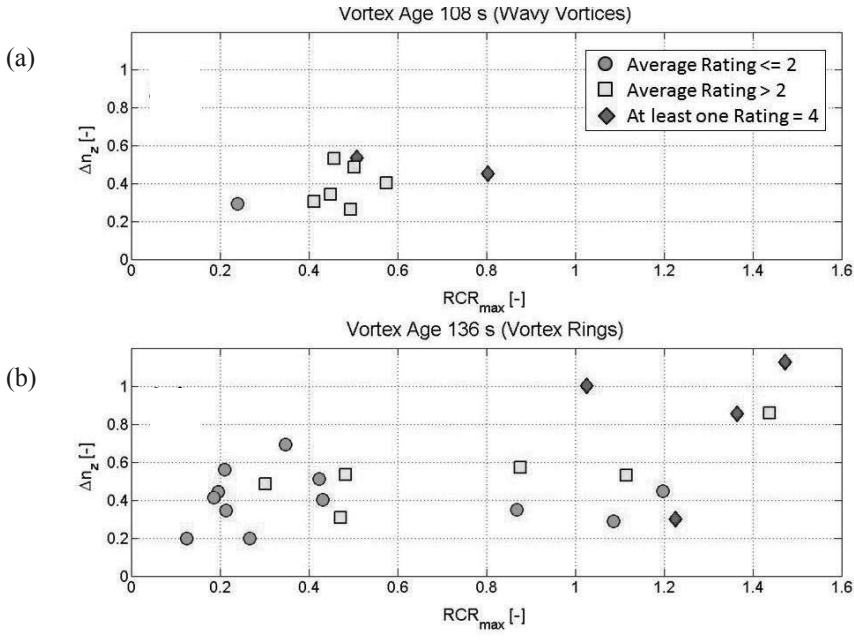


Figure 15. Resulting maximum vertical load factor during encounters with wavy vortices (a) and vortex rings (b).

The analysis of the roll rate shows that below a roll rate of approximately 15° to 17° there are no unacceptable encounters for both wavy vortices and vortex rings. However, there are acceptable encounters with vortex rings during which relatively large roll rates occurred. This fact indicates that the roll rate might be not the only factor for the pilot ratings.

The bank angle shows a similar correlation to the pilot ratings (Fig. 17). All unacceptable encounters show a maximum bank angle of at least 15°. Interestingly, some of the encounters with wavy vortices, which showed a large roll rate (Fig. 16) but were acceptable, are affected with relatively small bank angles (e.g. the encounter with vortex rings at RCR of about 1·2, Fig. 17). Probably a combination of bank angle and roll rate is the main measure for the pilot to rate the encounter hazard.

Generally speaking, one can say that the analysis of the in-flight simulation data indicates that also for less roll-dominated encounters with vortex rings, the roll-axis is the main axis for the pilots' hazard ratings. For this reason RCR is considered a meaningful metric also for wavy vortices.

As mentioned above, the results from the flight tests cannot serve as a basis for statistics due to the small number of conducted encounters. Nevertheless, the flight test results reveal interesting findings and in general support the results from previous investigations. Although the small amount of encounters with wavy vortices makes it difficult to determine a quantitative boundary, the results are not inconsistent with previous investigation. Concerning the harmlessness boundary, the results of the flight tests support the previously investigated acceptance boundary of RCR = 0·2, which was identified for straight vortices[22]. The previously mentioned simulator campaign in an A330 full-flight simulator[11] revealed that vortex deformation seems to increase the wake encounter hazard in manual flight. Against the background of those investigations with straight and deformed vortices, this flight test campaign with ATTAS cannot clearly correlate

https://doi.org/10.1017/S0001924000008654 Published online by Cambridge University Press

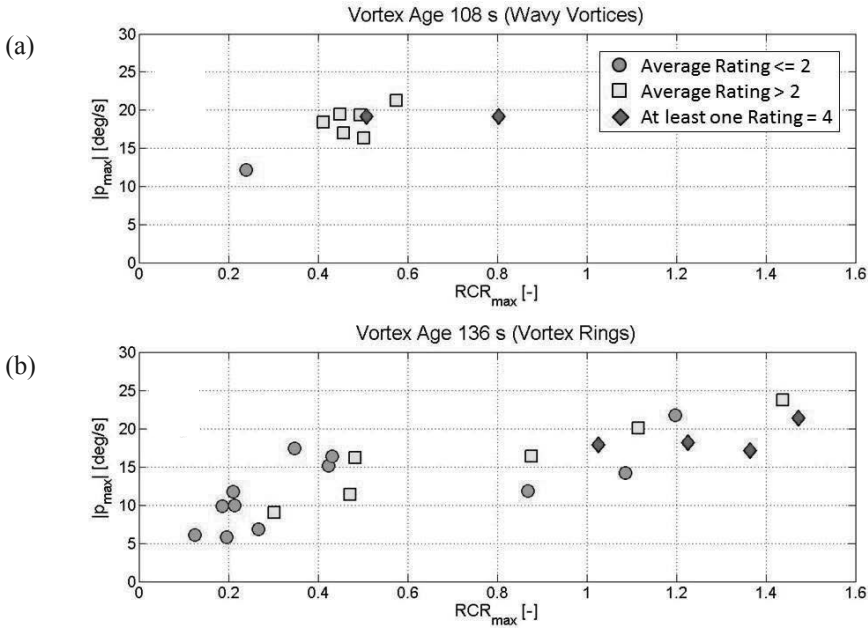


Figure 16. Resulting maximum roll rate during encounters with wavy vortices (a) and vortex rings (b).

vortex deformation and the encounter hazard. At least vortex rings might be considered as less dangerous by the pilots. However, the flight tests showed that encounters might be harmless below an RCR of 0·2 regardless of the degree of vortex deformation, which might be the most important outcome of this campaign.

5.0 CONCLUSION

In the framework of the DLR internal project 'Weather and Flying', the DLR Institute of Flight Systems have investigated the influence of wake vortex deformation on the encounter hazard. Flight tests with the DLR research aircraft ATTAS were performed for hazard assessment regarding vortex deformation using the in-flight simulation capability of ATTAS. The encounters were simulated in flight by applying vortex flow fields derived from large eddy simulations. Two different vortex ages were analysed, which represent different stages of vortex deformation, namely wavy vortices and vortex rings. The analysed scenario was of wake encounter during final approach. The encounters were rated by the pilots by means of a dedicated wake encounter rating scale, which was previously used for several piloted wake encounter hazard assessments. The pilot ratings were correlated with the roll control ratio RCR as a hazard severity metric, in order to serve as a basis for definition of an unacceptability boundary.

The results of the in-flight simulations indicate that, with small encounter angles, vortex deformation increases the impact of the wake encounter in all axes, not just the roll axis. While wavy vortices are predominantly associated with induced rolling motion, encounters with vortex rings are also associated with impacts in all other degrees of freedom. This can be observed by the analysis of the sideslip angle and vertical load factor. The pilot ratings show that pilots seem

https://doi.org/10.1017/S0001924000008654 Published online by Cambridge University Press

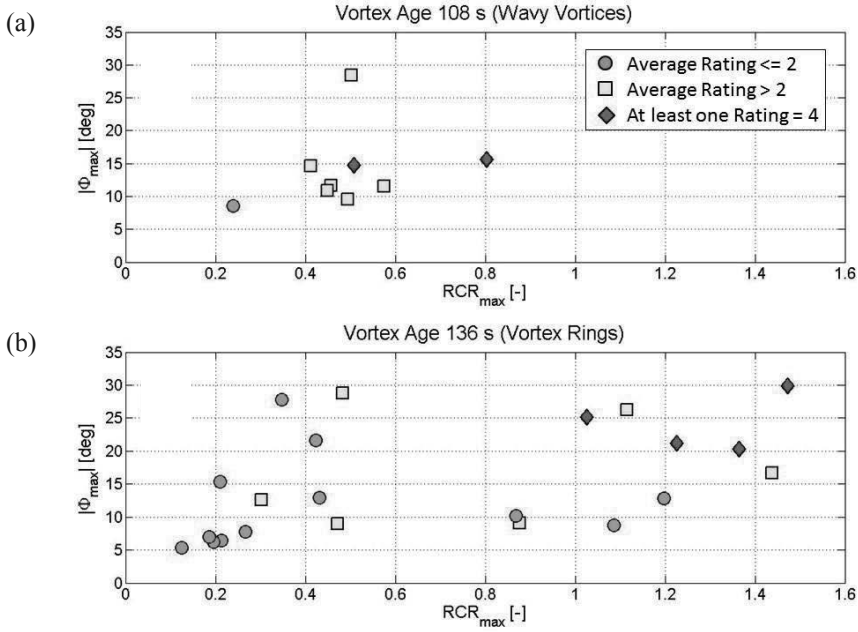


Figure 17. Resulting bank angle during encounters with wavy vortices (a) and vortex rings (b).

to assess those encounters as more dangerous which are dominated by induced rolling motion. The unacceptability boundary determined with the flight tests is at greater RCR values for encounters with vortex rings than for encounters with wavy vortices. The analysis of the flight test data also shows that the pilots seem to base their rating primarily on the aircraft reaction in the roll-axis. A correlation could be found between the pilot ratings and bank angle and roll rate but not clearly between the ratings and the sideslip angle or vertical load factor. Based on the pilot ratings, a second boundary, which is called the harmlessness boundary, was determined below which encounters seem to be negligible. Interestingly, this harmlessness boundary lies in the same region in terms of RCR for wavy vortices and vortex rings. For the stages of vortex deformation analysed in the in-flight simulations this boundary is in the range of RCR from 0·2 to 0·3.

The value of the harmlessness boundary supports previous investigation concerning encounter hazard with straight vortices of RCR = 0·2. The results of the investigation indicate that, possibly below a roll control ratio of RCR = 0·2, the influence of vortex deformation on the encounter hazard seems to be negligible. Above this boundary the influence of vortex deformation on encounter hazard could not finally be quantified yet and will be subject of further research.

Concluding, one can say that although the small amount of 31 encounters explored cannot serve as a basis for a wide understanding of the influence of vortex deformation on the encounter hazard, nevertheless some new outstanding results have been presented; namely that even though there is a higher pilot acceptance for those encounters which are less roll-dominated, pilots nevertheless base their hazard rating on the aircraft reaction in the roll axis. Also, the influence of vortex deformation on the encounter hazard seems to be negligible below an RCR of about 0·2.

https://doi.org/10.1017/S0001924000008654 Published online by Cambridge University Press

ACKNOWLEDGEMENTS

The author would like to thank his DLR colleagues Ingo Hennemann, who performed the large eddy simulations and Frank Holzäpfel from DLR Institute of Atmosperic Physics for their kind support and contributions. Special thanks are given to Dirk Leißling from DLR Institute of Flight Systems for the software implementation on ATTAS and to the flight crews from the DLR flight test facility in Braunschweig, namely the test pilots Hans-Jürgen Berns, Stefan Seydel, Andreas Hahn and Axel Widmann, as well as the flight test engineer Michael Press and the maintenance engineer Regina Gebhard.

REFERENCES

1. N.N. In-Flight Separation of Vertical Stabilizer American Airlines Flight 587 Airbus Industrie A300-605R N14053 Belle Harbor New York, USA, 12 November 2001, Aircraft Accident Report, NTSB/AAR-04/04, Washington, DC, USA, 2004.
2. N.N. Procedures for Air Navigation Services, Air Traffic Management, ICAO Doc 4444, 15th ed, 2007.
3. HOLZÄPFEL, F. *et al* Prediction of Dynamic Pairwise Wake Vortex Separations for Approach and Landing, AIAA Paper 2011-3037, AIAA Atmospheric Space Environments Conference, Honolulu, Hawaii, USA, 27-30 June 2011.
4. HAHN, K.-U. and SCHWARZ, C.W. Wake Vortex Avoidance versus Landing Capacity, AIAA Paper 2006-6322, AIAA Guidance, Navigation, and Control Conference, Keystone, Colorado, USA, 2006.
5. LOUCEL, R.E. and CROUCH, J.D. Flight-Simulator study of airplane encounters with perturbed trailing vortices, AIAA Paper 2004-1074, 42nd AIAA Aeospace Sciences Meeting and Exhibit, Reno, Nevada, USA, 2004.
6. REINKE, A. Evaluation of wake encounter flight tests in support of defining safe A380 separations, WakeNet3-Europe, 4th Major Workshop, Langen, Germany, March 2012.
7. HÖHNE, G., REINKE, A. and VERBEEK, M. Wake Vortex Encounter Flight Simulation: Metrics, Hazard Criteria, and Influence of Cockpit Motions, EU-project SWAKE, SWAKE-TN-320-1-v1, October 2002.
8. AMELSBERG, S. and KAUERTZ, S. Piloted Wake Vortex Encounter Simulator Tests for Departure, EU-project CREDOS Deliverable D, 3-4 November 2008.
9. HOLZÄPFEL, F. and GERZ, T. The DLR Project Wirbelschleppe: Detecting, Characterizing, Controlling, Attenuating, Understanding, and Predicting Aircraft Wake Vortices, DLR Research Report 2008-15, ISSN 1434-8454, 2008.
10. GERZ, T. and SCHWARZ, C. The DLR Project Wetter and Fliegen, DLR Research Report 2012-02, ISSN 1434-8454, 2012.
11. VECHTEL, D. Flight simulator study on the influence of vortex curvature on wake encounter hazard using les wind fields, *Aeronaut J*, March 2012, **116**, (177).
12. HENNEMANN, I. Deformation und Zerfall von Flugzeugwirbelschleppen in turbulenter und stabil geschichteter Atmosphäre (english: Deformation and Decay of Aircraft Wake Vortices in Turbulent and Stratified Atmosphere), Dissertation, Technical University Munich, 2010.
13. CROW, S.C. Stability theory for a pair of trailing vortices, *AIAA J*, 1970, **8**, (12), pp 2374-2381.
14. GERZ, T., HOLZÄPFEL, F. and DARRACQ, D. Commercial aircraft wake vortices, *Progress in Aerospace Sciences*, 2002, **38**, pp 181-208.
15. MISAKA, T. *et al* Vortex bursting and tracer transport of a counter-rotating vortex pair, *Physics of Fluids*, 2012, **24**, (2), pp 25104-1 – 25104-21.
16. HENNEMANN, I. Large-Eddy Simulation of Aircraft Wake Vortex Deformation and Topology, Proceedings of the Institute of Mechanical Engineers, *J Aerospace Engineering*, 2011, **225**, Part G.
17. KOLMOGOROV, A.N. The local structure of turbulence in incompressible viscous fluid for very large Reynolds numbers, *Dokl. AN SSSR*, 1941, **30**, (4), pp 299-303.
18. LAMB, H. *Hydrodynamics*, Cambridge University Press, pp 590-592, Cambridge, UK, 1932.
19. FRECH, M. *et al* High-resolution weather database for the terminal area of Frankfurt Airport, *J Applied Meteorology and Climatology*, November 2006, (46).
20. SCHWARZ, C.W. and HAHN, K.-U. Subjective Wake Vortex Encounter Evaluation, DLR Internal report IB 111-2011/46, Braunschweig, Germany, 2011.

https://doi.org/10.1017/S0001924000008654 Published online by Cambridge University Press

21. SAMMONDS, R.I. and STINNET jr, G.W. Hazard Criteria for Wake Vortex Encounters, NASA Technical Memorandum, NASA-TM-X-62473, Ames Research Center, Moffett Field, California, USA, 1975.
22. HAHN, K.-U. and SCHWARZ, C.W. Safe Limits for Wake Penetration, AIAA Paper 2007-6871, AIAA Guidance, Navigation and Control Conference and Exhibit, Hilton Head, South Carolina, 2007.
23. SCHWARZ, C.W. and VECHTEL, D. Wake Vortex Encounter Severity Criteria, WakeNet3-Europe Specific Workshop on Wake Vortex Encounter Severity Criteria, Braunschweig, 7 February 2012.
24. VAN DER GEEST, P. Wake Vortex Severity Criteria – The Search for a Single Metric, WakeNet3-Europe 4th Major Workshop on Wake Turbulence in Current Operations and Beyond, Langen, 28 February 2012.
25. HAHN, K.-U. Coping with Wake Vortex, 23rd International Congress of Aeronautical Sciences Proceedings, p 732.1-732.14, 2002.
26. SCHWARZ, C.W. and HAHN, K.-U. Full-flight simulator study for wake vortex hazard area investigation, Aerospace Science and Technology, **10**, pp 136-143, DOI 10.1016/j.ast.2005.09.005, 2006.
27. GESTWA, M., LEISSLING, D. and BAUSCHAT, J.-M. The Software Development Environment of the Flying Test-bed ATTAS, AIAA Paper 2005-6211, AIAA Modeling and Simulation Technologies Conference and Exhibit, San Francisco, California, USA, 15-18 August, 2005.
28. LEISSLING, D., GESTWA, M. and BAUSCHAT, J.-M. In-Flight Simulation in Support of an Aircraft Certification Process, AIAA Paper 2003-5532, AIAA Modeling and Simulation Technologies Conference and Exhibit, Austin, Texas, USA, 11-14 August, 2003.
29. HANKE, D. *et al*. In-Flight Simulator ATTAS – System Design and Capabilities, DGLR Congress, Paper No. DGLR 1991-05-02, 1991.
30. FISCHENBERG, D. A method to validate wake vortex encounter models from flight test data, ICAS 2010, 27th International congress of the aeronautical sciences, Nice, France, 2010.
31. BARROWS, T.M. Simplified Methods of Predicting Aircraft Rolling Moments due to Vortex Encounters, AIAA Paper 76-61, AIAA 14th Aerospace Sciences Meeting, Washington DC, USA, 1976.
32. DE BRUIN, A. WAVENC, Wake Vortex Evolution and Wake Vortex Encounter, Publishable Synthesis Report, National Aerospace Lab, NLR-TR-2000-079, Amsterdam, The Netherlands, 2000.
33. FISCHENBERG, D. Results of Flight Test Data Analysis, EU-project SWAKE, SWAKE-TN-222_1, 2002.
34. JATEGAONKAR, R., FISCHENBERG, D. and GRUENHAGEN, W.v. Aerodynamic Modelling and System Identification from Flight Data – Recent Applications at DLR, *J Aircr*, **41**, (4), p 687, 2004.

https://doi.org/10.1017/S0001924000008654 Published online by Cambridge University Press